J Incl Phenom Macrocycl Chem (2010) 66:357–364
DOI 10.1007/s10847-009-9653-3

ORIGINAL ARTICLE

Influence of the glucosylated β-cyclodextrin inclusion on sulfur trioxide spin-adduct stabilizations and spin-trapping rate processes for DMPO-type spin traps

Yoshimi Sueishi · Atsushi Miyata · Daisuke Yoshioka · Masato Kamibayashi · Yashige Kotake

Received: 19 April 2009 / Accepted: 20 July 2009 / Published online: 4 August 2009

Abstract The effect of CD-inclusion on spin-trapping rates and spin-adduct decay rates for sulfur trioxide radical anion ($SO_3^{-\bullet}$) was investigated. $SO_3^{-\bullet}$ radical was produced with UV photolysis of sodium sulfite in basic aqueous solution, and spin-trapped with various spin traps, i.e., PBN (α-phenyl-*N*-*t*-butylnitrone), DMPO (5,5-dimethyl pyrroline-1-oxide), and three other phosphoryl DMPO-type spin traps. A modified β-CD, 6-*O*-α-D-glucosyl-β-cyclodextrin (G-β-CD) having better inclusion properties than β-CD, was employed. Upon adding excess G-β-CD, decay rates of $SO_3^{-\bullet}$ radical adducts significantly decreased in most spin traps. Half-lives of $SO_3^{-\bullet}$ radical adducts of phosphoryl spin traps were one to two orders of magnitude longer than that of PBN or DMPO, and the G-β-CD addition further extended the half-life time. The spin traps containing phosphoryl-group all showed higher $SO_3^{-\bullet}$ trapping rates than those of PBN and DMPO, but two phosphoryl spin traps achieved slower trapping rates by G-β-CD addition. In addition, the structures of CD-inclusion complexes of spin traps were established by means of 1D and 2D NMR measurements. Based on the results, the influences of inclusion on the spin-trapping rate processes and spin-adduct stabilizations were discussed. We conclude that substituents in DMPO-type spin traps may be modified to provide best spin-trapping capabilities in the presence or absence of CD.

Keywords Spin trap · Inclusion complex · Cyclodextrin · ESR · NMR

Y. Sueishi (✉) · A. Miyata · D. Yoshioka
Department of Chemistry, Faculty of Science, Okayama University, 3-1-1 Tsushima-naka, Kita-ku, Okayama 700-8530, Japan
e-mail: ysueishi@cc.okayama-u.ac.jp

M. Kamibayashi
Kyoto Pharmaceutical University, Yamashina, Kyoto 607-8412, Japan

Y. Kotake
Free Radical Biology and Aging Research Program, Oklahoma Medical Research Foundation, Oklahoma City, OK 73104, USA

Introduction

Spin trapping is a convenient technique for the detection and identification of unstable free radicals [1, 2]. Nitrone and nitroso compounds have been most widely used as spin-trapping compounds in chemical and biological systems. Many investigators have attempted the design of spin traps giving more persistent spin adducts and a greater spectral resolution between the spin adducts, while further investigations seem to be necessary to obtain better results [3, 4].

Cyclodextrins are water-soluble oligosaccharides which form inclusion complexes with a large number of organic and inorganic molecules [5, 6]. Recently, Karoui and Tordo have shown that the inclusion complexation of PBN- and DMPO-superoxide spin adducts with β-cyclodextrin (CD) resulted in a significant stabilization of the spin adduct [7–10]. Free radicals included into the CD cavities may be defended from other reactants that shorten their lifetimes. CD-inclusion is considered as one of the means to improve spin-trapping capabilities, thus it is instructive to study how the spin adducts are stabilized by inclusion complexation with CD. Further, the influence of CD-inclusion on the spin trapping rates has not been well established.

Sulfur dioxide and various sulfites are used as preservatives and sanitizing agent in the food industry and are recognized as safe; however the sulfur-center trioxide radical anion ($SO_3^{-\bullet}$) which is formed during sulfite metabolism via one-electron oxidation, is proposed to contribute the mechanisms of toxicity [11]. Previously, the short-lived $SO_3^{-\bullet}$ radical has been investigated with spin trapping technique, using nitrone spin traps such as DMPO, but the half-life of $SO_3^{-\bullet}$ radical adduct of PBN or DMPO was short (<70 s) [12]. In this study, we investigated the stabilization mechanism of $SO_3^{-\bullet}$ radical adducts by inclusion-complexation by employing an inclusion-capability enhanced CD, 6-*O*-α-D-glucosyl-*β*-cyclodextrin (G-*β*-CD) [13]. Further, we have determined the $SO_3^{-\bullet}$ spin-trapping rates for three phosphorus-containing DMPO-type spin traps, including notable spin traps DPPMPO and CYPMPO in addition to PBN and DMPO. We also investigated the influence of CD-inclusion on the spin-tapping rate processes by these spin traps.

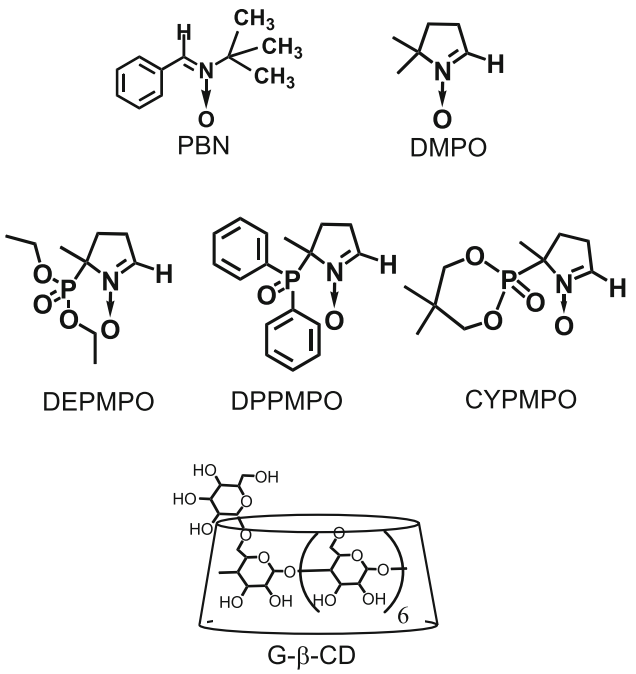

Fig. 1 Structures of PBN, DMPO, and phosphoryl DMPO analogs. *Bottom* figure is the schematic structure of glucosylated *β*-CD

Experimental

Materials and reagents

Spin traps illustrated in Fig. 1 were used in the present study: *N*-benzylidene-*t*-butylamine *N*-oxide (PBN), 5,5-dimethyl-pyrroline *N*-oxide (DMPO), 5-diethoxy-phosphoryl-5-methyl-1-pyrroline *N*-oxide (DEPMPO), 5-diphenylphosphoryl-5-methyl-1-pyrroline *N*-oxide (DPPMPO), and 5-(2,2-dimethyl-1,3-propoxyl cyclophosphoryl)-5-methyl-1-pyrroline *N*-oxide (CYPMPO). PBN and DMPO were purchased from Wako Pure Chemicals (Osaka, Japan). DEPMPO and DPPMPO were obtained from Radical Research Inc. (Hino, Japan) and Dojindo Laboratory (Kumamoto, Japan), respectively. CYPMPO was prepared according to the method reported by Kamibayashi et al. [14]. Sodium sulfite (Wako Pure Chemicals) was used as a source of sulfite anion trioxide radical ($SO_3^{-\bullet}$). To study the effect of inclusion on the spin-adduct stabilizations and spin-trapping rate processes, we used modified *β*-CD (6-*O*-α-D-glucosyl-*β*-cyclodextrin (G-*β*-CD)). G-*β*-CD is effective for the inclusion of ionic spin adducts, because G-*β*-CD has high water-solubility and high encapsulation ability [15]. $KHCO_3$/NaOH buffer was used in all spin trapping experiments.

ESR measurements of spin adducts

The $SO_3^{-\bullet}$ radical was generated with UV irradiation of sodium sulfite aqueous solution: 5 s irradiation with 200 W mercury arc (RUVF-203S, Radical Research Inc. Hino, Japan). In order to determine spin trapping rates in the presence of G-*β*-CD, we used a competitive spin trapping method, where two spin traps (e.g., DMPO and CYPMPO) compete each other to trap free radicals [16]. Typical experimental condition was as follows: Sodium sulfite (4.0×10^{-2} mol dm^{-3}), and spin traps (e.g., [DMPO] = 2.0×10^{-3} mol dm^{-3} and [CYPMPO] = 1.8×10^{-3} mol dm^{-3}) were mixed in $KHCO_3$/NaOH buffer (pH = 9.5), and loaded in the ESR flat cell. After UV light was in situ irradiated to the sample cell inside the cavity, ESR signals were immediately recorded with a JEOL JES-FE3XG ESR spectrometer: Sweep time 30 s, time constant 0.1 s, microwave power 5 mW. In competitive trapping method, ESR spectra of two different spin adducts were computer-simulated with the aid of an attached computer program (WIN-RAD computer system, Radical Research Inc.) by adjusting the relative intensity of two radical adducts. The relative abundance of the adduct components was calculated with a computer-mediated double-integration routine of the first-derivative signal of each component.

In order to elucidate the structure of the G-*β*-CD inclusion complex with spin traps, NMR spectra were measured in D_2O with a Varian Mercury 300 NMR spectrometer (300 MHz) at room temperature. Chemical shifts were reported as *δ* values relative to HOD (*δ* 4.79) as an internal standard [17]. 2D ROESY-NMR experiment was recorded at 600 MHz in D_2O on a Varian Inova AS600 NMR spectrometer at 303 K. Mixing times for ROESY experiments were set at 100 ms.

Results and discussions

Stabilization of spin adducts by CD inclusion complexation

By using NMR and ESR spectroscopy, Potapenko et al. identified the products of the nucleophilic addition of sulfite anions to the double bond of DMPO [18], suggesting the necessity of cautious analysis of $SO_3^{-\bullet}$ radical spin trapping data which are obtained in solutions containing sulfite anion and spin traps. Therefore, we carefully selected the experimental conditions. They suggested that keeping solution pH higher than 8.0 is an important factor to restrain the addition reaction [18]. Based on the results, we conducted the $SO_3^{-\bullet}$ radical trapping experiments under the basic condition of pH = 9.5.

Spin trapping of $SO_3^{-\bullet}$ radical anion by PBN, DMPO and phosphoryl DMPO-analogs (DEPMPO, DPPMPO, and CYPMPO (see, structures in Fig. 1) was performed with UV-irradiation of a sodium sulfite solution. Figure 2a and d show the ESR spectra of $SO_3^{-\bullet}$ radical adducts of DMPO and CYPMPO, respectively. The hyperfine structure (hfs) of the ESR spectra was assigned to splitting due to the nitrogen, hydrogen, and phosphorus atoms. These ESR spectra were readily reproduced by computer spectrum simulation (Fig. 2a, d). The spectral parameters (hyperfine coupling constants (hfcc's)) of DMPO adduct (A_N = 1.453 mT, A_H = 1.615 mT) agreed with the previous data for S-centered $SO_3^{-\bullet}$ radical adduct [19]. Hfcc's that were obtained in this work from other spin traps are listed in Table 1. The radical adducts of phosphorus-containing spin traps show characteristic large hfcc's of phosphorous nucleus.

Figure 2b and c show the ESR spectra of DMPO–$SO_3^{-\bullet}$ adducts in the presence of G-β-CD. In the presence of increasing amount of G-β-CD, ESR spectra changed from Fig. 2a to c, indicating the formation of the inclusion complex with G-β-CD. The ESR spectrum of Fig. 2b can be reproduced by computer simulation by superimposing two sets of six-line spectrum due to one nitrogen and hydrogen nucleus as illustrated in Fig. 2. In Fig. 2c, the ESR spectrum for only the inclusion complex of the DMPO–$SO_3^{-\bullet}$ adduct

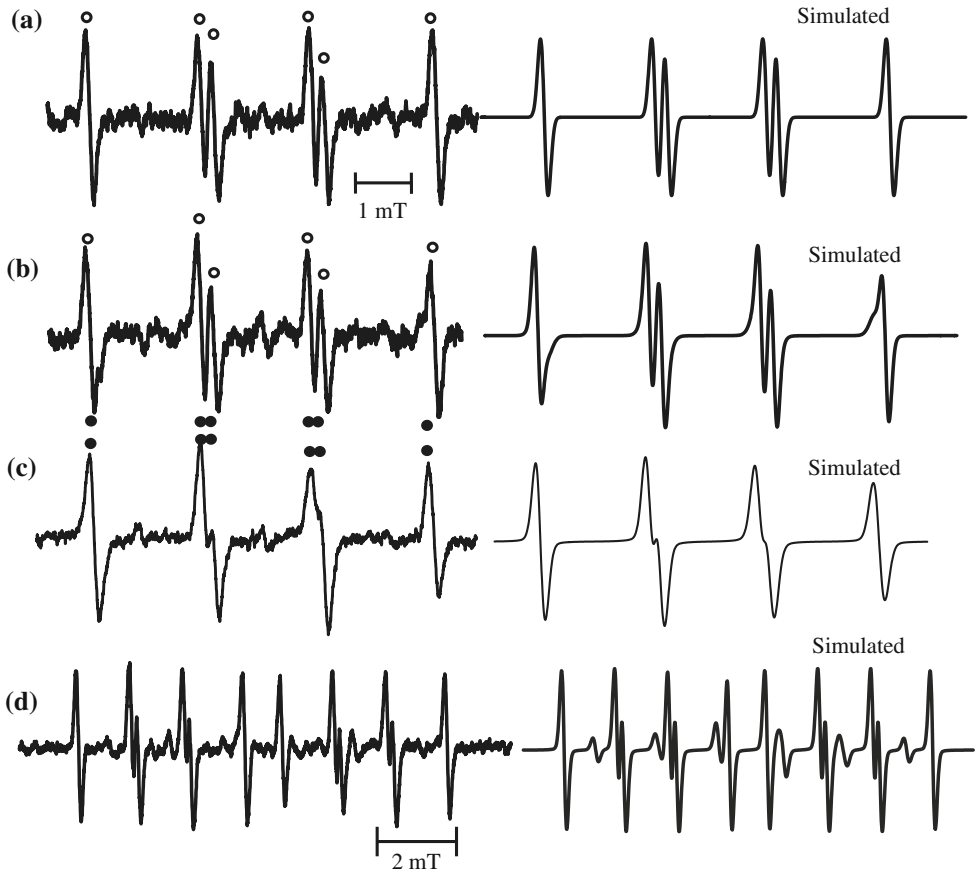

Fig. 2 ESR spectra of **a–c** DMPO–$SO_3^{-\bullet}$ and **d** CYPMPO–$SO_3^{-\bullet}$ adducts in the presence of various concentrations of G-β-CD: **a–c** $[DMPO]_0 = 1.79 \times 10^{-3}$ mol dm^{-3}. $[G\text{-}\beta\text{-}CD]_0$ = **a** 0, **b** 1.79×10^{-3}, and **c** 99.0×10^{-3} mol dm^{-3}. The peaks marked with open circles and closed circles are assigned to DMPO–$SO_3^{-\bullet}$ adduct and its inclusion complex, respectively. **d** $[CYPMPO]_0 = 0.92 \times 10^{-3}$ mol dm^{-3}

Table 1 Hyperfine coupling constants, decay-rate constants, and half-lives of $SO_3^{-\bullet}$ spin adducts

Traps	A_N/mT	A_H/mT	A_P/mT	10^3 k/s^{-1}	$t_{1/2}$/s	$t_{1/2}^{CD}/t_{1/2}$
DMPO	1.453	1.615	–	9.5 ± 0.2	73	–
DMPO + G-β-CD[a]	1.422	1.552	–	2.4 ± 0.1	290	4.0
PBN	1.498	0.197	–	67 ± 1	10	–
PBN + G-β-CD[b]	1.488	0.237	–	25 ± 1	28	2.8
DEPMPO	1.358	1.521	5.002	1.9 ± 0.2	370	–
DEPMPO + G-β-CD[c]	1.304	1.304	5.005	0.43 ± 0.02	1600	4.4
DPPMPO	1.294	1.497	3.812	0.61 ± 0.02	1100	–
DPPMPO + G-β-CD[d]	1.280	1.412	3.972	0.30 ± 0.01	2300	2.0
CYPMPO[e]	1.328, 1.550	1.499, 1.640	5.100, 3.080	0.40 ± 0.02	1700	–
CYPMPO + G-β-CD[e,f]	1.220, 1.330	1.370, 1.490	4.940, 4.860	0.40 ± 0.01	1700	1.0

[a] $[\text{G-}\beta\text{-CD}]_0/[\text{DMPO}]_0 = 101$ and $[\text{DMPO}]_0 = 1.0 \times 10^{-3}$ mol dm^{-3}; [b] $[\text{G-}\beta\text{-CD}]_0/[\text{PBN}]_0 = 20$ and $[\text{PBN}]_0 = 7.0 \times 10^{-3}$ mol dm^{-3}; [c] $[\text{G-}\beta\text{-CD}]_0/[\text{DEPMPO}]_0 = 250$ and $[\text{DEPMPO}]_0 = 1.0 \times 10^{-3}$ mol dm^{-3}; [d] $[\text{G-}\beta\text{-CD}]_0/[\text{DPPMPO}]_0 = 100$ and $[\text{DPPMPO}]_0 = 3.0 \times 10^{-3}$ mol dm^{-3}; [e] The two diastereomeric spin adducts are shown; [f] $[\text{G-}\beta\text{-CD}]_0/[\text{CYPMPO}]_0 = 80$ and $[\text{CYPMPO}]_0 = 1.0 \times 10^{-3}$ mol dm^{-3}

could be observed in the solution of high G-β-CD concentrations ($[\text{G-}\beta\text{-CD}]_0/[\text{DMPO}]_0 = 55$).

The hfcc's for the inclusion complexes of spin adducts with G-β-CD are listed in Table 1. A large decrease in A_N occurred when the spin adduct for DMPO, DEPMPO or CYPMPO was included in G-β-CD cavity, indicating that the N–O group is surrounded by less polar environment than in water. The inner wall of the CD cavity is known to be less polar than water, suggesting that the N–O group is encapsulated in the CD cavity.

We determined decay rates of $SO_3^{-\bullet}$ radical adducts of PBN and four DMPO-type spin traps (Table 1). The decay of the $SO_3^{-\bullet}$ radical adduct was monitored with the intensity decrease in the low-field ESR line, and was analyzed according to first-order kinetics. The decay well followed first-order kinetics and we calculated the rate constants (k) and half-life times ($t_{1/2}$) for spin adducts. As shown in Fig. 2c, the all spin adducts in the solution of high G-β-CD concentrations exist as the inclusion complex, though G-β-CD favors the inclusion of the neutral spin traps than the ionic spin adducts of the $SO_3^{-\bullet}$ radical. Therefore, in great excess of CD ($[\text{G-}\beta\text{-CD}]_0/[\text{traps}]_0 > 60$), we can assume that the all molecules of spin traps and adducts are included in the CD cavity and the spin adduct is not in an in-and-out inclusion equilibrium. In fact, the effect of the excess CD-concentration on the decay rates of the $SO_3^{-\bullet}$ radical adducts was not observed. The rate constants and $t_{1/2}$ values for the decay of spin adducts are listed in Table 1, together with those in the presence of G-β-CD. The half-life of ESR signal of the $SO_3^{-\bullet}$ radical adducts of PBN extended from 10 s to 28 s by CD-inclusion (Table 1). DMPO-type spin traps produced persistent $SO_3^{-\bullet}$ radical adducts with half-lives ranging from 73 s to 1700 s, indicating that the inclusion by G-β-CD enhanced spin adducts' stability. In particular, the stabilization effects, i.e. the ratio $t_{1/2}^{CD}/t_{1/2}$, with the CD inclusion are outstanding for DMPO and DEPMPO (Table 1). The structural change by CD-inclusion may be responsible for such change (see "Inclusion complexes of spin traps"). It is likely that free radicals included by CD cavity are defended from other reactants that shorten their lifetime. In addition, the molecular motion that could promote decomposition of free radicals may be restricted in the narrow CD cavity. It is interesting to note that $SO_3^{-\bullet}$ radical adduct of CYPMPO already showed a long half-life (1700 s), but CD addition had no effect on the half-life. We speculate that electronic or spacious structure of CYPMPO spin adduct is already optimized to provide maximum stability without CD-inclusion.

Competitive spin trapping of $SO_3^{-\bullet}$ radical anion

We employed competitive spin-trapping between two distinctive spin traps to determine the rate constants for $SO_3^{-\bullet}$ radical trapping [16]. Figure 3 shows the typical ESR spectrum obtained in UV-irradiated solution of sodium sulfite in the presence of both DMPO and CYPMPO. DMPO–$SO_3^{-\bullet}$ adduct showed the hfcc of $A_N = 1.453$ mT and $A_H = 1.615$ mT and CYPMPO–$SO_3^{-\bullet}$ adduct showed two species having hfcc's of [$A_N = 1.328$ mT $A_H = 1.499$ mT and $A_P = 5.100$ mT] and [$A_N = 1.550$mT $A_H = 1.640$ mT and $A_P = 3.080$ mT]. The two species are assigned to diastereomers of CYPMPO–$SO_3^{-\bullet}$ adducts. The multiple component ESR spectrum was reproduced by computer spectrum simulation and the relative abundance of the spin adducts by two spin traps (DMPO and CYPMPO) were calculated using the simulated each component. The following is the reaction scheme for spin trapping in the presence of two spin traps (for example, DMPO and CYPMPO):

$$SO_3^- \xrightarrow{h\nu} SO_3^{-\bullet}$$

$$DMPO + SO_3^{-\bullet} \rightarrow DMPO{-}SO_3^{-\bullet} \quad k_{DMPO}$$

$$CYPMPO + SO_3^{-\bullet} \rightarrow CYPMPO{-}SO_3^{-\bullet} \quad k_{CYP}$$

The ratio of the formation rates for CYPMPO–$SO_3^{-\bullet}$ and DMPO–$SO_3^{-\bullet}$ adducts can be expressed as follows:

$$\frac{R_{CYP}}{R_{DMPO}} = \frac{d\left[CYPMPO{-}SO_3^{-\bullet}\right]/dt}{d\left[DMPO{-}SO_3^{-\bullet}\right]/dt} = \frac{k_{CYP}\ [CYPMPO]_0}{k_{DMPO}\ [DMPO]_0} \tag{1}$$

where $[CYPMPO]_0$ and $[DMPO]_0$ denote the initial concentrations of spin traps. The relative trapping rate constants (k_{CYP}/k_{DMPO}) can be calculated from the relative rates of spin-adduct formation (the relative abundance of spin adducts) and the initial concentrations of spin traps.

A typical plot for the CYPMPO/DMPO system is shown in Fig. 3c with a straight line passing through the origin, suggesting that the trapping-reaction mechanism is justifiable. The calculated relative rate constants (k_{CYP}/k_{DMPO}) are listed in Table 2. The previously determined DMPO spin-trapping rate of $SO_3^{-\bullet}$ radical was $k_{DMPO} = 1.2 \times 10^7$ dm^3 mol^{-1} s^{-1} [20], and this value was used to calculate the $SO_3^{-\bullet}$ radical trapping rate constants for the present spin traps (Table 2). These values indicate that the DMPO-analogs have high trapping efficiency for the $SO_3^{-\bullet}$ radical as compared with PBN.

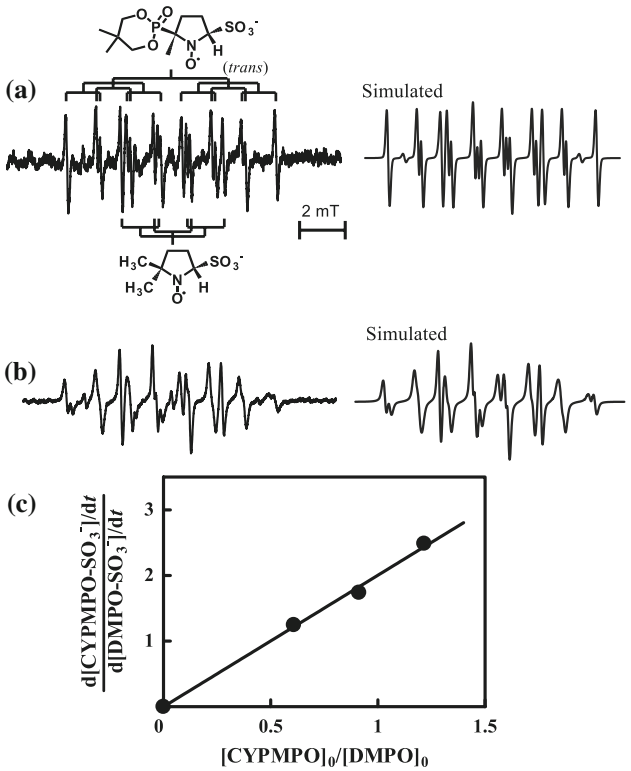

Fig. 3 ESR spectra obtained immediately after UV-irradiation in the presence of DMPO and CYPMPO, and computer-simulated spectra: **a** $[CYPMPO]_0/[DMPO]_0 = 0.92$ and $[CYPMPO]_0 = 0.92 \times 10^{-3}$ mol dm^{-3}. **b** $SO_3^{-\bullet}$ radical anion trapping in the presence of excess G-β-CD: $[CYPMPO]_0/[DMPO]_0 = 1.8$, $[CYPMPO]_0 = 1.25 \times 10^{-3}$ mol dm^{-3} and $[G\text{-}\beta\text{-CD}]_0 = 0.10$ mol dm^{-3}. **c** The ratio of $SO_3^{-\bullet}$ adduct formation rates for CYPMPO and DMPO plotted as a function of the initial concentration of spin traps ($[CYPMPO]_0/[DMPO]_0$): The formation rate of CYPMPO adducts was calculated from the sum of two diastereomeric spin adducts

The influence of CD-inclusion on the spin-trapping rate is an interesting topic in reaction kinetics. Figure 3b shows the ESR spectrum of the competing spin adducts of DMPO and CYPMPO in the presence of excess G-β-CD. Using ESR parameters for inclusion complexes in Table 1, the ESR spectrum could be reproduced by superimposing ESR spectra of inclusion complexes of DMPO and CYPMPO radical adducts (Fig. 3b). As suggested above, in large excess of G-β-CD, the all spin-trap and -adduct molecules may be encapsulated in the CD cavity and thus, the similar reaction scheme to the competitive spin-trapping in excess CD can be proposed as follows:

$$SO_3^- \xrightarrow{h\nu} SO_3^{-\bullet}$$

$$DMPO(CD) + SO_3^{-\bullet} \rightarrow DMPO(CD){-}SO_3^{-\bullet} \quad k_{DMPO}{}^{CD}$$

$$CYPMPO(CD) + SO_3^{-\bullet} \rightarrow CYPMPO(CD){-}SO_3^{-\bullet} \quad k_{CYP}{}^{CD}$$

where DMPO(CD) and CYPMPO(CD) denote the inclusion complexes of DMPO and CYPMPO with G-β-CD, respectively. DMPO(CD)–$SO_3^{-\bullet}$ and CYPMPO(CD)–$SO_3^{-\bullet}$ are the G-β-CD inclusion complexes of DMPO and CYPMPO spin-adducts. In large excess of G-β-CD, the ratio of DMPO(CD)–$SO_3^{-\bullet}$ and CYPMPO(CD)–$SO_3^{-\bullet}$ formation can be given by

$$\begin{aligned}\frac{R_{CYP}{}^{CD}}{R_{DMPO}{}^{CD}} &= \frac{d\left[CYPMPO(CD){-}SO_3^{-\bullet}\right]/dt}{d\left[DMPO(CD){-}SO_3^{-\bullet}\right]/dt} \\ &= \frac{k_{CYP}{}^{CD}\ [CYPMPO(CD)]_0}{k_{DMPO}{}^{CD}\ [DMPO(CD)]_0} \\ &= \frac{k_{CYP}{}^{CD}\ [CYPMPO)]_0}{k_{DMPO}{}^{CD}\ [DMPO)]_0}\end{aligned} \tag{2}$$

As predicted by Eq. 2, the plot of $R_{CYP}{}^{CD}/R_{DMPO}{}^{CD}$ (the relative abundance of CYPMPO and DMPO adducts) against $[CYPMPO]_0/[DMPO]_0$ gives the relative trapping rate constants $k_{CYP}{}^{CD}/k_{DMPO}{}^{CD}$ values for the inclusion complexes of spin traps, and these values are listed in Table 2. In the presence of excess CD, the $k^{CD}/k_{DMPO}{}^{CD}$ values for PBN and DPPMPO are large compared with those in the absence of CD; however the $k^{CD}/k_{DMPO}{}^{CD}$ values for DEPMPO and CYPMPO are smaller than those in absence of CD. In connection with the structures of the inclusion complexes of spin traps, details on the trapping rate changes caused by the inclusion into CD will be discussed below.

Table 2 Trapping rate constants for $SO_3^{-\bullet}$ radical anion at 298 K in aqueous solution

Spin traps	Ratio of spin trapping rate constants	Absolute trapping rate constants/dm^3 mol^{-1} s^{-1} [a]	$k_{DMPO\text{-}traps}/k_{PBN}$, $k_{DMPO\text{-}traps}{}^{CD}/k_{PBN}{}^{CD}$
PBN/DMPO[b]	0.0295 ± 0.0010	$k_{PBN} = 0.035 \times 10^7$	34 (DMPO/PBN)
PBN/DMPO + G-β-CD[c]	0.0552 ± 0.0016	–	18 (DMPO/PBN + G-β-CD)
DEPMPO/DMPO[d]	1.46 ± 0.02	$k_{DEPMPO} = 1.8 \times 10^7$	49 (DEPMPO/PBN)
DEPMPO/DMPO + G-β-CD[e]	1.37 ± 0.03	–	25 (DEPMPO/PBN + G-β-CD)
DPPMPO/DMPO[f]	1.21 ± 0.01	$k_{DPPMPO} = 1.5 \times 10^7$	41 (DPPMPO/PBN)
DPPMPO/DMPO + G-β-CD[g]	2.73 ± 0.07	–	49 (DPPMPO/PBN + G-β-CD)
CYPMPO/DMPO[h]	2.01 ± 0.06	$k_{CYPMPO} = 2.4 \times 10^7$	68 (CYPMPO/PBN)
CYPMPO/DMPO + G-β-CD[i]	1.11 ± 0.01	–	20 (CYPMPO/PBN + G-β-CD)

[a] $k_{DMPO} = 1.2 \times 10^7$ dm^3 mol^{-1} s^{-1} [Cited from Ref. 20] is used; [b] $[DMPO]_0 = 1.0 \times 10^{-3}$ mol dm^{-3}; [c] $[DMPO]_0 = 1.0 \times 10^{-3}$ mol dm^{-3} and $[G\text{-}\beta\text{-}CD]_0/[DMPO]_0 = 100$; [d] $[DEPMPO]_0 = 2.0 \times 10^{-3}$ mol dm^{-3}; [e] $[DEPMPO]_0 = 0.7 \times 10^{-3}$ mol dm^{-3} and $[G\text{-}\beta\text{-}CD]_0/[DEPMPO]_0 = 250$; [f] $[DPPMPO]_0 = 6.0 \times 10^{-3}$ mol dm^{-3}; [g] $[DPPMPO]_0 = 3.0 \times 10^{-3}$ mol dm^{-3} and $[G\text{-}\beta\text{-}CD]_0/[DPPMPO]_0 = 100$; [h] $[CYPMPO]_0 = 0.92 \times 10^{-3}$ mol dm^{-3}; [i] $[CYPMPO]_0 = 1.3 \times 10^{-3}$ mol dm^{-3} and $[G\text{-}\beta\text{-}CD]_0/[CYPMPO]_0 = 80$

Inclusion complexes of spin traps

^{1}H-NMR measurements have been shown to be informative to elucidate the guest–host molecular position in inclusion complex because the induced chemical shifts of the guest protons indicate an inclusion of the proton moiety into the CD cavity [21]. We determined induced changes of the chemical shifts of PBN, DMPO, DPPMPO and CYPMPO in the presence of G-β-CD in D_2O (Fig. 4). Summary of the result is: (1) In PBN, large chemical shift changes for C(7)–H and $–CH_3$ protons are observed, compared with those of the benzene ring protons, indicating the inclusion of G-β-CD occurred from the *t*-butyl group side; and (2) In DMPO, the induced chemical shift values of $–CH_3$ and C(3)–H moiety are large compared with the others, suggesting that the $>C(CH_3)_2$ and C(3)–H moieties are deeply inserted into the CD cavity. The inspection of the Corey–Pauling–Koltun (CPK) space-filling model seems to show that the double bond (radical trap site) in DMPO is included in the G-β-CD cavity. Such form of inclusion may be responsible for the large stabilization effect on the spin adducts. Judging from the effects of inclusion on the half-life of spin-adduct decays, the large $t_{1/2}{}^{CD}/t_{1/2}$ for DEPMPO spin adduct (Table 1) suggests that the inclusion occurred from the pyrroline ring side. In contrast, the small stabilization effects on the decays of DPPMPO and CYPMPO spin-adducts suggest the different inclusion aspects for the spin adducts. In fact, in DPPMPO large chemical shift changes for C(7,8)–H on the benzene ring are observed. In CYPMPO, the induced chemical shift values of the protons in the cyclophosphoryl ring are larger than those on the pyrroline ring. These chemical shifts demonstrate that DPPMPO and CYPMPO are encapsulated into the G-β-CD cavity from the phenyl-group side and the $>C(CH_3)_2$ side of the cyclophosphoryl ring moiety, respectively.

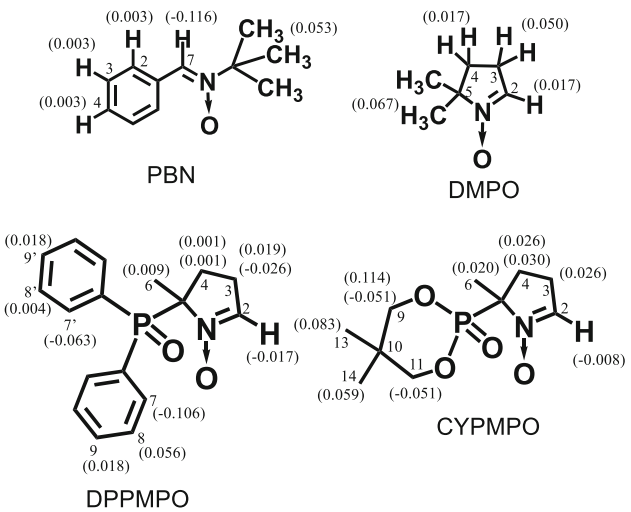

Fig. 4 Induced chemical shifts (Δδ (ppm) in parentheses) of the ^{1}H NMR protons of PBN, DMPO, DPPMPO, and CYPMPO upon inclusion complexation with G-β-CD: $[G\text{-}\beta\text{-}CD]_0/[PBN]_0 = 2.4$, $[G\text{-}\beta\text{-}CD]_0/[DMPO]_0 = 2.4$, $[G\text{-}\beta\text{-}CD]_0/[DPPMPO]_0 = 1.1$, and $[G\text{-}\beta\text{-}CD]_0/[CYPMPO]_0 = 1.2$. $\Delta\delta = \delta(\text{complex}) - \delta(\text{free})$. A negative value indicates an upfield shift

There is a significant difference in the effects of inclusion on the trapping-rate ratios for DPPMPO and CYPMPO. We conducted the detailed discussion on the structures of inclusion complexes with these two traps. The 2D ROESY-NMR experiments are instructive for the discussion on the position of the guest molecule in the CD cavity. Figure 5 shows the ROESY-NMR spectra of DPPMPO/G-β-CD and CYPMPO/G-β-CD in D_2O solution and the cross-peaks were detected between the inner protons (H-3 and H-5) of the G-β-CD cavity and guest molecules of DPPMPO and CYPMPO. In DPPMPO, the cross-peaks of C(8)–H proton on the benzene ring of DPPMPO with the H-3,5 protons of G-β-CD were detected, and those between C(7)–H proton and H-3 proton of CD appeared;

however, the cross-peaks arising from the H-3,5 protons of CD with the C(2,3,4,6)-H protons of DPPMPO were not observed, which confirmed the inclusion of the benzene ring of DPPMPO by G-β-CD. In CYPMPO, the cross-peaks between C(2,3,4)–H protons of CYPMPO and H-3,5 protons of G-β-CD were not detected, while those between C(9,11,13,14)–H protons and H-3,5 protons of G-β-CD appeared as can be seen in Fig. 5. Further, since the interaction between the C(6)–H proton in CYPMPO and the H-3 proton of CD can be seen, the cyclophosphoryl ring moiety is deeply encapsulated into the CD cavity, which is responsible for the decelerated effect on the trapping rate of CYPMPO included by G-β-CD.

When comparing $SO_3^{-\bullet}$ spin-trapping rates within DMPO-analogs, it is informative to express the relative trapping rate constants with respect to PBN spin-trapping rate because PBN's radical-trapping site is located outside the CD cavity (on the CD rim), thus k/k_{PBN} and $k^{CD}/k_{PBN}{}^{CD}$ values are given in the right-hand side column of Table 2. The calculation of these values allowed us to make interesting discussion: In DPPMPO, the $k^{CD}/k_{PBN}{}^{CD}$ value is comparable to that in the absence of CD; however, in DMPO, DEPMPO and CYPMPO these values are smaller than those in the absence of CD, meaning free-radical trapping capabilities are diminished by CD inclusion in these spin traps. It is possible to interpret that in DMPO, DEPMPO and CYPMPO the nitrone trapping site is shielded from radical species. As suggested above, because of phenyl-group inclusion, the nitrone trapping site in DPPMPO is exposed even after inclusion.

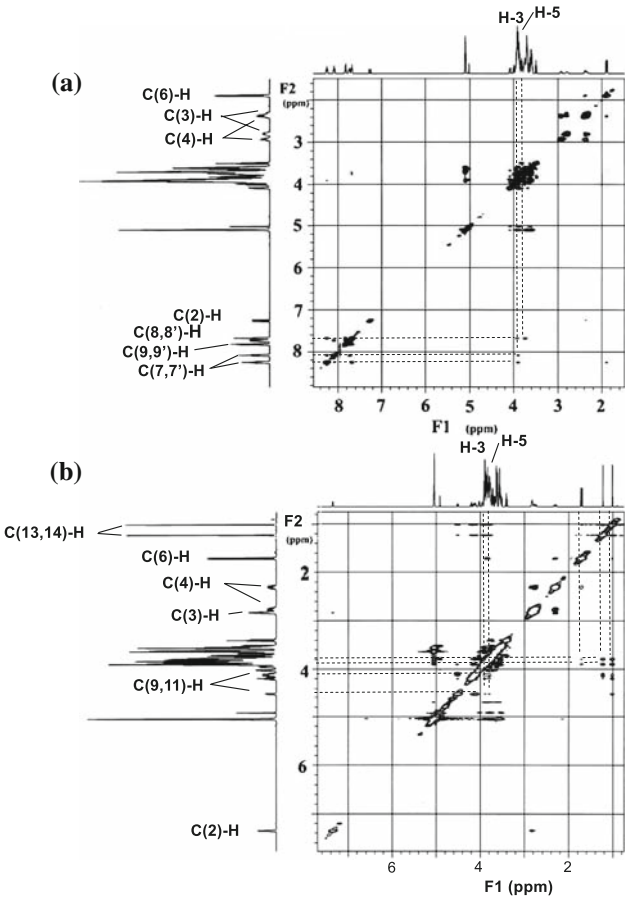

Fig. 5 2D ROESY-NMR spectra (100 ms mixing time) at 303 K in D_2O solutions in which **a** $[G\text{-}\beta\text{-}CD]_0/[DPPMPO]_0 = 1.1$ and **b** $[G\text{-}\beta\text{-}CD]_0/[CYPMPO]_0 = 1.2$

In conclusion, we were able to make a comprehensive description of structural and dynamic aspects of the influence of CD presence for $SO_3^{-\bullet}$ spin trapping reaction. This may help in the structural design of better spin traps in the future.

References

1. Janzen, E.G.: Spin trapping. Acc. Chem. Res. **4**, 31–40 (1971)
2. Buettner, G.R.: Spin trapping: ESR parameters of spin adducts. Free Rad. Biol. Med. **3**, 259–303 (1987)
3. Bacic, G., Spasojevic, I., Secerov, B., Mojovic, M.: Spin-trapping of oxygen free radicals in chemical and biological systems: new traps, radicals and possibilities. Spectrochim. Acta A **69**, 1354–1366 (2008)
4. Hardy, M., Rockenbauer, A., Vasquez-Vivar, J., Felix, C., Lopez, M., Srinivasan, S., Avadhni, N., Tordo, P., Kalyanaraman, B.: Detection, characterization, and decay kinetics of ROS and thiyl adducts of mito-DEPMPO spin trap. Chem. Res. Toxicol. **20**, 1053–1060 (2007)
5. Li, S., Purdy, W.C.: Cyclodextrins and their applications in analytical chemistry. Chem. Rev. **92**, 1457–1470 (1992)
6. Sueishi, Y., Tobisako, H., Kotake, Y.: Group-inclusion complex and its external high pressure effect on O-methylated β-cyclodextrin as compared with unmodified β-cyclodextrin. Bull. Chem. Soc. Jpn. **80**, 894–898 (2007)
7. Karoui, H., Tordo, P.: ESR-spin trapping in the presence of cyclodextrins. Detection of PBN-superoxide spin adduct. Tetrahedron Lett. **45**, 1043 (2004)
8. Karoui, H., Rockenbauer, A., Pietri, S., Tordo, P.: Spin trapping of superoxide in the presence of β-cyclodextrins. Chem. Commun. 3030–3031 (2002)
9. Bardelang, D., Rockenbauer, A., Karoui, H., Finet, J.-P., Tordo, P.: Inclusion complexes of PBN-type nitrone spin traps and their superoxide spin adducts with cyclodextrin derivatives: parallel detection of the association constants by NMR titrations and 2D-EPR simulations. J. Phys. Chem. B **109**, 10521–10530 (2005)
10. Bardelang, D., Rockenbauer, A., Karoui, H., Finet, J.-P., Biskupska, I., Banaszak, K., Tordo, P.: Inclusion complexes of EMPO derivatives with 2, 6-di-O-methyl-β- cyclodextrin: synthesis, NMR and EPR investigations for enhanced superoxide detection. Org. Biomol. Chem. **4**, 2874–2882 (2006)
11. Rabinowitch, H.D., Rosen, G.M., Fridovich, I.: A mimic of superoxide dismutase activity protects Chlorella sorokiniana against the toxicity of sulfite. Free Rad. Biol. Med. **6**, 45–48 (1989)
12. Mottley, C., Mason, R.P.: Sulfate anion free radical formation by the peroxidation of (bi)sulfite and its reaction with hydroxyl radical scavengers. Arch. Biochem. Biophys. **267**, 681–689 (1985)

13. Sueishi, Y., Inazumi, N., Hanaya, T.: NMR spectroscopic characterization of inclusion complexes of hydroxy-substituted naphthalenes with native and modified β-cyclodextrins. J. Incl. Phenom. Macrocycl. Chem. **64**, 135–141 (2009)
14. Kamibayashi, M., Oowada, S., Kameda, H., Okada, T., Inanami, O., Ohta, S., Ozawa, T., Makino, K., Kotake, Y.: Synthesis and characterization of a practically better DEPMPO-type spin trap, 5-(2, 2-dimethyl-1, 3-propoxyl cyclophosphoryl)-5-methyl-1-pyrroline N-oxide (CYPMPO). Free Rad. Res. **40**, 1166–1172 (2006)
15. Koizumi, K., Okada, Y., Kubota, Y., Utamura, T.: Inclusion complexes of poorly water-soluble drugs with glucosyl-cyclodextrins. Chem. Pharm. Bull. **35**, 3413–3418 (1987)
16. Sueishi, Y., Yoshioka, D., Yoshioka, C., Yamamoto, S., Kotake, Y.: High static pressure alters spin trapping rates in solution. Dependence on the structure of nitrone spin traps. Org. Biomol. Chem. **4**, 896–901 (2006)
17. Gottlieb, H.E., Kotlyar, V., Nudelman, A.: NMR chemical shifts of common laboratory solvents as trace impurities. J. Org. Chem. **62**, 7512–7515 (1997)
18. Potapenko, D.I., Bagryanskaya, E.G., Reznikov, V.V., Clanton, T.L.: NMR and EPR studies of the reaction of nucleophilic addition of (bi)sulfite to nitrone spin trap DMPO. Magn. Reson. Chem. **41**, 603–608 (2003)
19. Mottley, C., Mason, R.P., Chignell, C.F., Sivarajah, K., Eling, T.E.: The formation sulfur trioxide radical anion during the prostaglandin hydroperoxidase-catalyzed oxidation of bisulfite (hydrated sulfur dioxide). J. Biol. Chem. **257**, 5050–5055 (1982)
20. Taniguchi, H., Madden, K.P.: An in situ radiolysis time-resolved ESR study of the kinetics of spin trapping by 5, 5-dimethyl-1-pyrroline-N-oxide. J. Am. Chem. Soc. **121**, 11875–11879 (1999)
21. Inoue, Y., Okada, T., Miyata, Y., Chujo, R.: N.M.R. study of cycloamylose inclusion-complexes with p-substituted phenols. Carbohydr. Res. **125**, 65–76 (1984)